

## Rotational bands in $^{113}\text{Sb}$

P. Banerjee,<sup>1</sup> S. Ganguly,<sup>2</sup> M. K. Pradhan,<sup>1</sup> H. P. Sharma,<sup>3</sup> S. Muralithar,<sup>4</sup> R. P. Singh,<sup>4</sup> and R. K. Bhowmik<sup>4</sup>

<sup>1</sup>*Saha Institute of Nuclear Physics, Sector 1, Block-AF, Bidhan Nagar, Kolkata 700 064, India*

<sup>2</sup>*Department of Physics, Chandernagore College, Chandernagore, Hooghly 712136, India*

<sup>3</sup>*Benaras Hindu University, Varanasi-221005, India*

<sup>4</sup>*Inter University Accelerator Centre, New Delhi 110067, India*

(Received 1 January 2013; published 25 March 2013)

Rotational bands in  $^{113}\text{Sb}$ , populated in the reaction  $^{100}\text{Mo}(^{19}\text{F},6n)$  at a beam energy of 105 MeV, have been studied. Two previously reported strongly coupled high- $K$  bands have been extended and a new sequence of five states, linked to the positive-parity high- $K$  band through interband transitions, is proposed. A comparison of the experimental  $B(M1)/B(E2)$  ratios for the latter band with the predictions of the geometrical model of Dönau-Frauentorf suggests that the states are axially symmetric with a moderate quadrupole deformation of  $\beta_2 = 0.20$ . Present directional correlation orientation and  $\gamma$ -ray polarization studies indicate that the negative-parity states built upon the 3045 keV isomeric level involve a high- $\Omega$   $\pi h_{11/2}$  orbital and have an oblate shape. Mean lifetimes for eight states belonging to the prolate-deformed  $\pi h_{11/2}$  band have been measured from Doppler shift attenuation data. The results suggest a large average quadrupole deformation of  $\beta_2 = 0.32 \pm 0.03$  for states up to 10217 keV. The decrease of the  $B(E2)$  rates for the 9063- and 10217 keV states may be interpreted as a signature of band termination at high spin.

DOI: [10.1103/PhysRevC.87.034321](https://doi.org/10.1103/PhysRevC.87.034321)

PACS number(s): 21.10.Re, 21.10.Tg, 25.70.Gh, 27.60.+j

### I. INTRODUCTION

The odd-mass Sb ( $Z = 51$ ) nuclei display diverse modes of excitations. While the low-energy states are mostly spherical and vibrational in nature, the ones at high energy have sizable collectivity. The spherical excitations are a manifestation of the proton shell closure at  $Z = 50$ ; the odd proton in the  $g_{7/2}$ ,  $d_{5/2}$ , and  $h_{11/2}$  orbitals couple to the spherical Sn core to form these states. Collective states in these nuclei have been interpreted to arise from either (i) a two-particle-one-hole ( $2p$ - $1h$ ),  $\pi(g_{7/2}, d_{5/2})^2 \otimes \pi(g_{9/2})^{-1}$  configuration, resulting from the excitation of a  $g_{9/2}$  proton across the  $Z = 50$  shell gap and leading to  $\Delta J = 1$  bands, or (ii) the coupling of the odd proton in the  $h_{11/2}$ ,  $g_{7/2}$ , and  $d_{5/2}$  orbitals to the  $2p$ - $2h$  deformed Sn core states giving rise to  $\Delta J = 2$  decoupled sequences. Multiple deformed  $\Delta J = 1$  bands have been observed in  $^{111,113,115,117}\text{Sb}$  based on the high- $K$ ,  $\beta$ -upsloping  $\pi g_{9/2}$  orbital and characterized by little or no signature splitting. The  $\Delta J = 2$  structures involving a valence proton coupled to deformed Sn cores are best exemplified in the midshell nucleus  $^{117}\text{Sb}$  [1], where three such bands have been reported based on protons in the  $d_{5/2}$ ,  $g_{7/2}$ , and  $h_{11/2}$  orbitals. Janzen *et al.* [2] have reported a  $\Delta J = 2$  band in  $^{113}\text{Sb}$  based on a  $\pi h_{11/2}$  orbital up to an excitation energy of 21.1 MeV and spin  $(79/2^-)$  (the last state is tentative). A large average quadrupole deformation of  $\beta_2 \simeq 0.32$  has been reported in the literature for this band [2,3]. A characteristic feature of this and similar bands in this mass region is a large decrease in their dynamic moment of inertia ( $\zeta^{(2)}$ ), to approximately a third of the rigid-body value, as the rotational frequencies approach 1 MeV/ $\hbar$ . Moreover, lifetime studies in  $^{109}\text{Sb}$  have shown a smooth decline in  $B(E2)$  values with spin for the higher-lying states [4]. This has been interpreted as owing to a gradual change in the shape of the nucleus from collective prolate at low spins to noncollective oblate at high spins, associated with the alignment of the

angular momentum vectors of the valence nucleons with the rotational axis.

The primary objective of the present work is to study the structure of rotational bands in  $^{113}\text{Sb}$ . Part of the work on  $^{113}\text{Sb}$  populated in the reaction  $^{100}\text{Mo} + ^{20}\text{Ne}$  at a beam energy of  $E = 136$  MeV, using six clover detectors, has been previously reported [3]. The present work relates to the results obtained from a recent experiment with a more efficient detector system comprising 15 clover detectors. Most of the previously reported collective bands have been extended to higher spins and a significant revision has been made in the level scheme for several bands. In addition, an interpretation of the  $\pi h_{11/2}$  intruder band is attempted on the basis of a remeasurement of the lifetimes of the levels belonging to this band. Present polarization directional correlation orientation (PDCO) studies also lead to a better understanding of some of the bands.

### II. EXPERIMENTAL METHOD

Excited states of  $^{113}\text{Sb}$  were populated in the  $^{100}\text{Mo}(^{19}\text{F},6n)$  reaction at a beam energy of  $E = 105$  MeV at the 15UD Pelletron Accelerator at the Inter University Accelerator Centre (IUAC), New Delhi. Isotopically enriched (99.5%)  $^{100}\text{Mo}$  with a thickness of 2 mg/cm<sup>2</sup>, evaporated on a 8 mg/cm<sup>2</sup> gold foil formed the target. The experiment yielded about  $25 \times 10^9$  two- and higher-fold coincident events using the Indian National Gamma Array (INGA) comprising 15 Compton-suppressed clover detectors. Four of these detectors were placed at 90° and 148° each, three at 32°, and two each at 57° and 123° to the beam direction.

Gated spectra with a dispersion of 0.5 keV per channel were generated from  $4096 \times 4096$  matrices, obtained from the sorting of the gain-matched raw data. The symmetric  $E_\gamma$ - $E_\gamma$

matrix was used for determining the  $\gamma$ -ray coincidence relationships and building the level scheme. Spectra for lifetime analyses using the Doppler shift attenuation (DSA) technique were generated from matrices formed from coincidences between either the backward ( $148^\circ$ ) or the forward ( $32^\circ$ ) angle events with those in the remaining detectors. However, the backward angle spectra were used in most cases as there were fewer detectors in the forward angle. The directional correlation of oriented nuclei (DCO) ratios for assignment of  $\gamma$ -ray multipolarity was determined, as outlined in Ref. [5], from a matrix with events recorded at  $90^\circ$  along one axis and those at  $148^\circ$  along the other. Two other matrices were used for PDCO ratios. One of these was built from events recorded in the segments of the  $90^\circ$  clover detector that were perpendicular to the emission plane and the other parallel to it, respectively, in coincidence with events recorded in all the other detectors. The data were analyzed using the computer codes INGASORT [6] and the Radware packages ESCL8R and SLICE [7].

The lifetimes of the excited states were extracted using the analysis package LINESHAPE [8]. The slowing down history of the recoils (moving with an initial recoil velocity of  $\beta = 0.017$ ) in the target and backing were simulated using a Monte Carlo technique, which involved 10000 histories with a time step of 0.002 ps and the results sorted according to detector geometry. The shell-corrected stopping powers of Northcliffe-Schilling [9] were used. The fitting process was started with the highest observed transition in the band with adequate statistics and continued progressively for the transitions deexciting the lower-lying states. The level lifetimes were corrected for both discrete feedings from the higher-energy states and direct feedings from the continuum. The direct feeding times were assumed to be similar to those used for  $^{111}\text{In}$ , reported in Ref. [5]. The relative intensities of the feeding transitions were determined from gated spectra observed at  $57^\circ$  and  $123^\circ$  to the beam direction. Errors stated in the transition quadrupole moments  $Q_t$  and level lifetimes ( $\tau$ ) include the statistical uncertainties in the data and the effects of an assumed 50% uncertainty in the direct feeding times.

The two asymmetric PDCO matrices were used to determine the electromagnetic nature (electric or magnetic) of the  $\gamma$ -rays. The asymmetry of the Compton scattered photons were obtained from the relation

$$A = \frac{aN_{\perp} - N_{\parallel}}{aN_{\perp} + N_{\parallel}},$$

where  $N_{\perp}$  and  $N_{\parallel}$  denote the number of  $\gamma$ -rays with scattering axis perpendicular and parallel, respectively, to the emission plane and  $a$  is the correction factor owing to the asymmetry in the response of the segments of the clover detector, defined as

$$a = \frac{N_{\parallel}}{N_{\perp}}.$$

The correction factor  $a$ , measured as a function of the  $\gamma$ -ray energy, has a value close to unity. A positive (negative) value of the asymmetry term  $A$  corresponds to a pure stretched electric (magnetic) transition while for mixed transitions, the asymmetry factor is close to zero.

### III. EXPERIMENTAL RESULT

The level scheme of  $^{113}\text{Sb}$  deduced from the present work is shown in Fig. 1. Levels up to 19146 keV have been observed. Most of the states (except the low-energy spherical ones) have been grouped into five bands as shown. Bands 1 and 5 are together populated with about 24%, Band 2 with 32%, and Band 3 with 38% of the channel intensity. The residual intensity goes into Band 4, which is the weakest of all. The placement of the transitions in the different bands have been made on the basis of  $\gamma\gamma$ -coincidence data. Selected gated spectra are shown in Figs. 2 and 3. Tables I and II summarize the important experimental results obtained in the present work. These are discussed in the following sections.

#### A. Bands 1 and 5

The strongly coupled, positive parity band (Band 1) was first reported by Moon *et al.* [10]. Considerable revision of the level scheme has resulted from the present work. Two new states at 4763 and 7485 keV and five transitions with energies 399, 508, 678, 848, and 939 keV have been added to the band as shown in Fig. 1. Besides, the ordering of the 389 and 425 keV  $\gamma$ -rays has been changed.

There are several transitions in Band 1 which are nearly degenerate in energy and are observed in self-gated projected spectra. The placements of the new 399 and 848 keV transitions deexciting the 4763 keV level in Band 1 is supported by the observation of these  $\gamma$ -rays in the spectra gated by the lower-lying transitions in the band. The spectrum gated by the 309 keV transition is shown in Fig. 2(a). It may be noted here that a previously reported [10] 398 keV transition and a new 847 keV  $\gamma$ -ray also deexcite the 2308 keV level in Band 5. However, the latter  $\gamma$ -rays are not expected to be observed in the spectrum gated by the 309 keV transition. Also, the self-gated spectra with gates on 398 and 847 keV  $\gamma$ -rays lend support to the placements of the new 399, 847, and 848 keV  $\gamma$ -rays. The new 678 keV  $\gamma$ -ray, connecting the 5042- and 4364 keV levels, is weak. However, it is observed in all spectra gated by transitions belonging to Band 1 except the 296 and 382 keV gates. The 296 keV gate [Fig. 2(b)] shows the 939 keV crossover transition deexciting the new 7485 keV level as well as all the other crossover  $E2$  transitions in the band. The inset in Fig. 2(b) shows an expanded region of the same spectrum in support of the placement of the new 508 keV transition at the top of the band.

In addition, the placements of the 389 and 425 keV transitions have been interchanged (Fig. 1) with respect to the level scheme reported earlier [10]. This interchange replaces the previously reported [10] 3084 keV state by the new 3049 keV state. Indeed, the 3049 keV state is found to decay to the 2308 keV level in Band 5 by a new 741 keV transition [see Fig. 2(b)] and provides firm support for interchanging the placements of the two  $\gamma$ -rays. Both Shroy *et al.* [11] and Janzen *et al.* [2] have also reported the same ordering of the 389 and 425 keV transitions as proposed in this work.

Band 5 is a new sequence of five states with energies 2308, 2722, 3113, 3401, and 3749 keV, connected by the 414, 391, 288, and 348 keV transitions. Of these, the 391 and 288 keV  $\gamma$ -rays were reported earlier in Ref. [10]. The sequence is shown

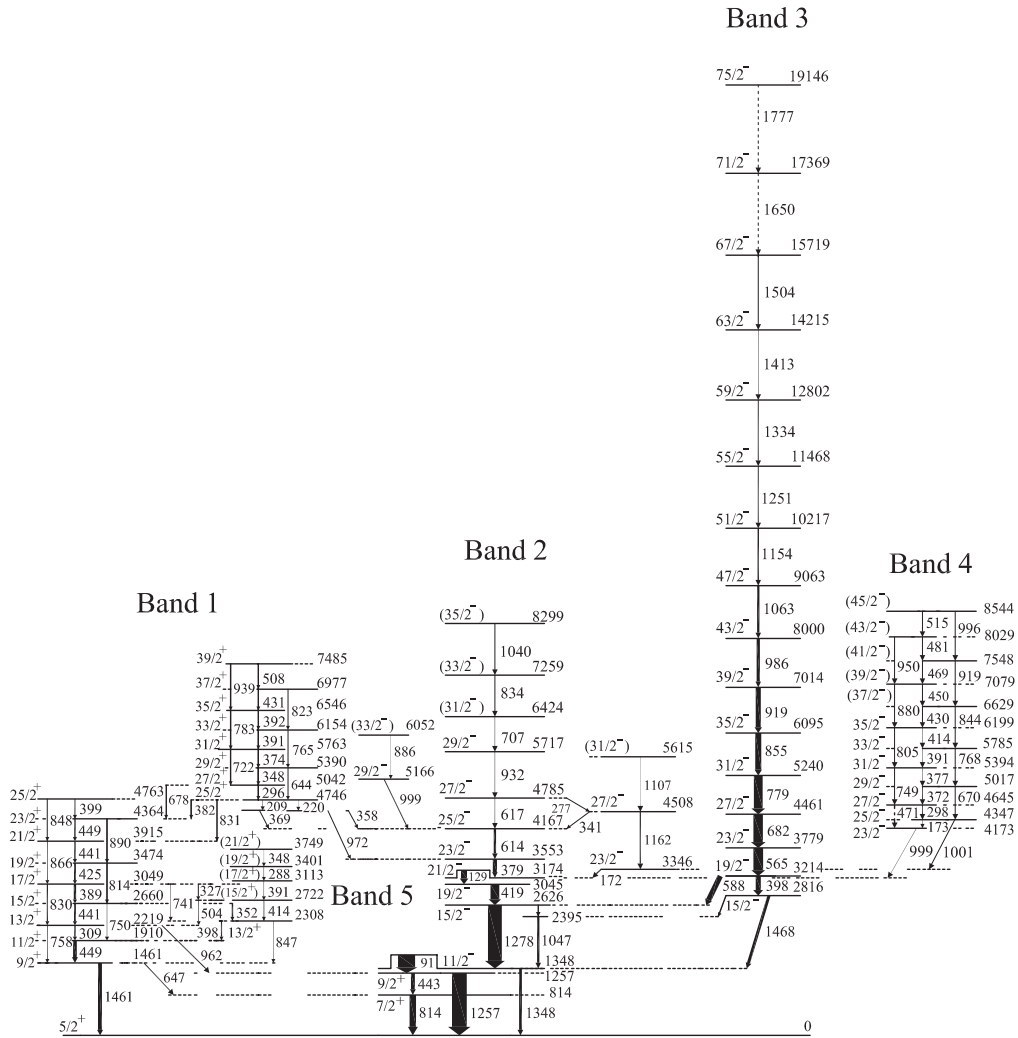


FIG. 1. Partial level scheme of  $^{113}\text{Sb}$  based on the present work. The level and  $\gamma$ -ray energies are given in keV. The relative intensities of the transitions are indicated by the widths of the arrows.

to be connected to Band 1 through six transitions with energies 327, 352, 398, 504, 741, and 847 keV. The 352, 398, and 504 keV  $\gamma$ -rays have been reported previously but were placed differently [10]. The other three placements in Band 5 and the interband transitions are supported by the spectra gated by the 288, 398, and 504 keV  $\gamma$ -rays. Figure 2(c) shows the spectra gated by the 288 keV  $\gamma$ -ray.

The adopted spins and parities ( $J^\pi$ ) reported in the literature [12] for levels up to an excitation energy of 4364 keV belonging to Band 1 are indicated as tentative although Moon *et al.* [10] have reported firm  $J^\pi$  assignments for all these states. These assignments are consistent with the earlier angular distribution measurements of Shroy *et al.* [11]. The present DCO measurements confirm the spin-parity assignments of Moon *et al.* [10]. The  $\gamma$ -ray multipole mixing ratios  $\delta$  for the  $\Delta J = 1$  transitions (Table I), estimated from the present  $R_{\text{DCO}}$  values, lie in the range 0.02–0.42, indicating  $E2$  admixtures of up to 15%. The  $R_{\text{DCO}}$  values for the 309, 374, and 449 keV  $\gamma$ -rays, estimated from gating on the 1461 keV

$E2$  transition, are close to unity and suggest that the transitions could be quadrupole in nature. However, this is ruled out as parallel crossover  $E2$  transitions are already established in the band (Fig. 1). The  $R_{\text{DCO}}$  values for these transitions only lead to sizable  $E2$  admixtures in their multipolarity (Table I). The present  $\delta$  values are in agreement with those reported by Shroy *et al.* [11], except for the 309 keV transition for which the present  $\delta = 0.34 \pm 0.08$  is larger by a factor of two. The new 4763 keV level is assigned a  $J^\pi$  of  $25/2^+$  on the basis of a  $M1/E2$  multipolarity assignment for the 399 keV transition (see Table I). Although DCO measurements could not be made for the 848 keV  $\gamma$ -ray, the presence of this crossover transition gives further support to this spin assignment.

The adopted  $J^\pi$  values [12] for the states of the aligned sequence with energies  $\geq 4746$  keV are the same as those assigned by Moon *et al.* [10], although the basis for the latter assignments is not clear in the absence of supporting data. Results of present DCO measurements for the 296, 348, 374, and 431 keV  $\gamma$ -rays are given in Table I. These results are consistent with the adopted  $J^\pi$  assignments [12].

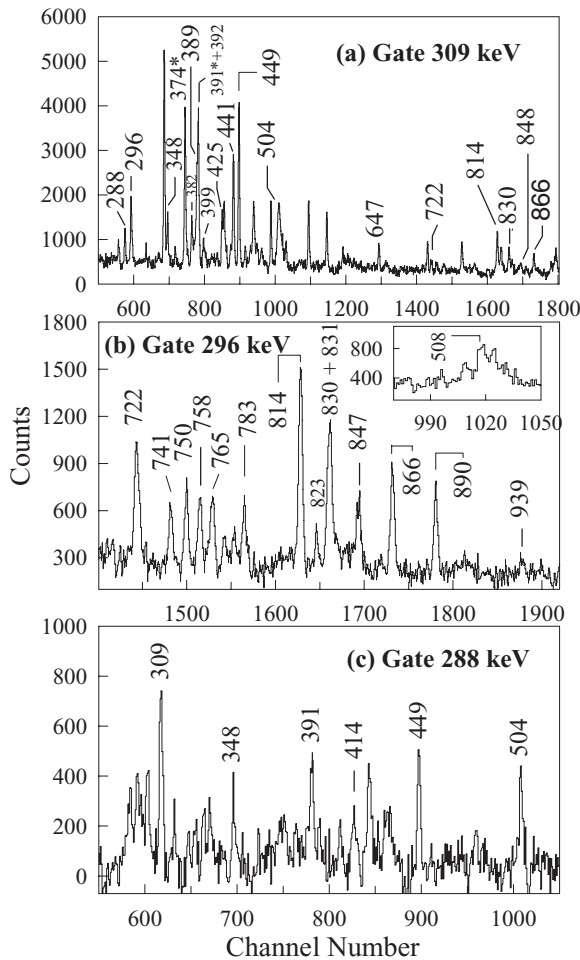


FIG. 2. Prompt  $\gamma$ - $\gamma$  coincidence spectra gated by (a) 309 keV, (b) 296 keV, and (c) 288 keV transitions belonging to Bands 1 and 5. Transitions belonging to only these two bands are marked.  $\gamma$ -rays indicated with an asterisk belong to  $^{114}\text{Sb}$ . The inset in (b) shows a part of the spectrum gated by the 296 keV  $\gamma$ -ray.

However, DCO measurements for the 391, 392, and the new 508 keV transitions could not be made. Nevertheless, firm  $J^\pi$  assignments are proposed for all states in this sequence, including the new 7485 keV state, as shown in Fig. 1, on the basis of the systematics of the band.

The spin and parity of the 2308 keV state in Band 5 is tentatively adopted as  $(13/2^+)$  in the literature [12]. The new 847 keV  $\gamma$ -ray from this level, feeding the  $9/2^+$  state in Band 1, is found to be quadrupole in nature in the present work (Table I). This confirms the spin of  $13/2^+$  for the 2308 keV level. The DCO results for the 352 and 398 keV transitions connecting the 2308 keV state to Band 1 are consistent with this assignment. However, the four higher-energy states at 2722, 3113, 3401, and 3749 keV in this sequence could not be assigned firm spins owing to insufficient statistics in the DCO data.

### B. Band 2 and the low energy states

Band 2 is built upon the  $19/2^-$  isomeric state at 3045 keV with a half-life of  $T_{1/2} = 3.7 \pm 0.3$  ns [12]. The band,

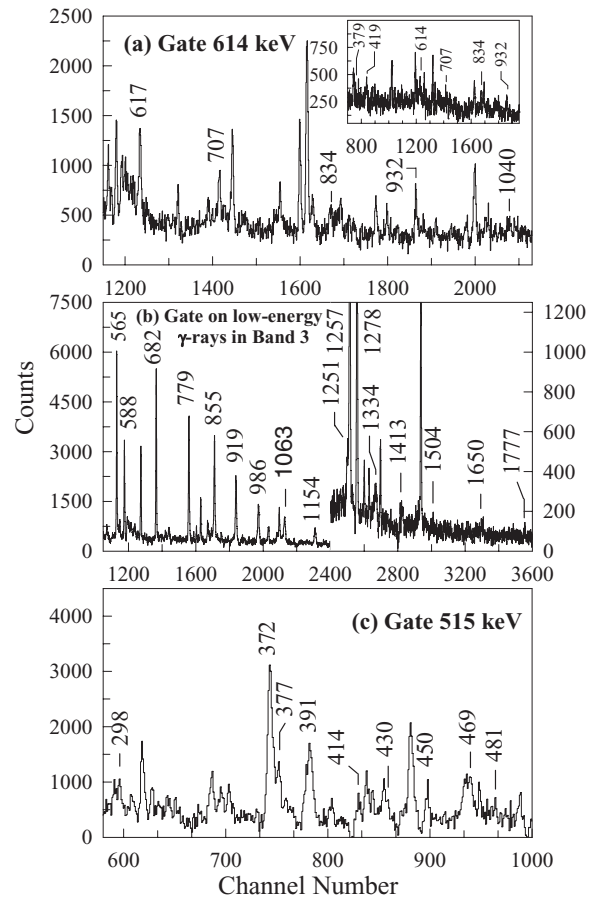


FIG. 3. Prompt  $\gamma$ - $\gamma$  spectra with gates on (a) 614 keV transition in Band 2, (b) sum of the  $\gamma$ -ray spectra gated by the low-energy transitions up to 855 keV in Band 3, and (c) 515 keV transition belonging to Band 4. The inset in (a) shows a part of the spectrum gated by the 1040 keV transition in Band 2.

previously reported up to 6424 keV, has been extended by the addition of two new levels up to an excitation energy of 8299 keV and a tentative spin of  $(35/2^-)$  (Fig. 1). Placement of the new 834 and 1040 keV transitions is based on the observation of these  $\gamma$ -rays in spectra gated by the lower-lying transitions in the band. Figure 3(a) shows the spectrum gated by the 614 keV  $\gamma$ -ray. The inset in Fig. 3(a) displays the spectrum gated by the new 1040 keV transition, showing all the lower-energy  $\gamma$ -rays in the band.

Firm spin and parities have been reported for all states up to the bandhead at 3045 keV by Moon *et al.* [10], although the adopted results [12] show the  $J^\pi$  for the 2626 keV and the parity of the 3045 keV states as unconfirmed. The present DCO and PDCO measurements for the 1278 and 419 keV  $\gamma$ -rays (Table I) confirm the  $J^\pi$  for the 2626 and 3045 keV states as reported in Ref. [10]. The next higher-energy level at 3174 keV, deexciting by the 129 keV transition, is also assigned a tentative  $J^\pi = 21/2^{(-)}$  in the literature [12]. The present  $\delta = 0.15_{-0.05}^{+0.03}$  for the 129 keV  $\gamma$ -ray suggests that it is predominantly  $M1$  in nature and that the 3174 keV state also has a negative parity. A positive parity for this state and hence an  $E1$  assignment for the 129 keV transition would lead to an unrealistically large  $M2$  admixture. The four higher-lying

TABLE I. Present experimental results on level energies ( $E_x$ ),  $\gamma$ -ray energies ( $E_\gamma$ ),  $R_{\text{DCO}}$ , multipole mixing ratio  $\delta$ , and asymmetry ratios for  $^{113}\text{Sb}$ .

Band	$E_x$ (keV)	$E_\gamma$ (keV)	Gating transition (keV)	$R_{\text{DCO}}$	$\delta$ value	Asymmetry ratio	$J_i^\pi \rightarrow J_f^\pi$
1 and 5	1910	449	1461	$0.94 \pm 0.11^a$	$0.41 \pm 0.10$	–	$11/2^+ \rightarrow 9/2^+$
	2219	309	1461	$0.88 \pm 0.09$	$0.34 \pm 0.08$	–	$13/2^+ \rightarrow 11/2^+$
	2660	441	1461	$0.69 \pm 0.10^a$	$0.16 \pm 0.09$	–	$15/2^+ \rightarrow 13/2^+$
		352	1461	$0.75 \pm 0.14$	$0.21 \pm 0.10$	–	$15/2^+ \rightarrow 13/2^+$
	3474	425	1461	$0.70 \pm 0.11$	$0.16 \pm 0.11$	–	$19/2^+ \rightarrow 17/2^+$
	4763	399	309	$0.87 \pm 0.26$	$0.07 \pm 0.19$	–	$25/2^+ \rightarrow 23/2^+$
	5042	296	382	$1.24 \pm 0.11$	$0.42 \pm 0.23$	–	$27/2^+ \rightarrow 25/2^+$
	5390	348	382	$1.14 \pm 0.12$	$0.35 \pm 0.23$	–	$29/2^+ \rightarrow 27/2^+$
	5763	374	1461	$0.89 \pm 0.17$	$0.31 \pm 0.15$	–	$31/2^+ \rightarrow 29/2^+$
	6977	431	1461	$0.54 \pm 0.23$	$0.02 \pm 0.23$	–	$37/2^+ \rightarrow 35/2^+$
	2308	398	1461	$0.72 \pm 0.16$	$0.17 \pm 0.13$	–	$13/2^+ \rightarrow 11/2^+$
		847	1461	$0.94 \pm 0.37$	$-0.04 \pm 0.35$	–	$13/2^+ \rightarrow 9/2^+$
	2	3045	419	1278	$1.27 \pm 0.12$	$E2$	$0.26 \pm 0.07$
3174		129	419	$0.69 \pm 0.06$	$0.15^{+0.03}_{-0.05}$	–	$21/2^- \rightarrow 19/2^-$
3553		379	419	$0.37 \pm 0.02$	$-0.35^{+0.04}_{-0.06}$	$0.10 \pm 0.07$	$23/2^- \rightarrow 21/2^-$
4167		614	419	$0.44 \pm 0.04$	$-0.20^{+0.05}_{-0.07}$	$-0.07 \pm 0.12$	$25/2^- \rightarrow 23/2^-$
4785		617	419	$0.37 \pm 0.04$	$-0.36 \pm 0.11$	$-0.08 \pm 0.16$	$27/2^- \rightarrow 25/2^-$
5717		932	419	$1.06 \pm 0.14$	$0.54^{+0.32}_{-0.17}$	$\sim 0.02$	$29/2^- \rightarrow 27/2^-$
4		4347	1001	419	$0.61 \pm 0.10$	$0.06^{+0.09}_{-0.11}$	–
	5017	372	298	$1.10 \pm 0.21$	$0.04^{+0.14}_{-0.11}$	–	$29/2^- \rightarrow 27/2^-$
	5394	377	298	$0.88 \pm 0.20$	$0.18 \pm 0.13$	–	$31/2^- \rightarrow 29/2^-$
	5785	391	298	$1.14 \pm 0.27$	$0.08^{+0.14}_{-0.16}$	–	$33/2^- \rightarrow 31/2^-$
	6199	414	298	$0.91 \pm 0.09$	$0.05^{+0.05}_{-0.07}$	–	$35/2^- \rightarrow 33/2^-$
Other States	2626	1278	1257	$1.05 \pm 0.04$	$E2$	$0.10 \pm 0.07$	$15/2^- \rightarrow 11/2^-$
	3346	172	419	$0.73 \pm 0.10$	$0.17 \pm 0.10$	–	$23/2^- \rightarrow 21/2^-$
	4508	1162	419	$1.12 \pm 0.17$	$E2$	–	$27/2^- \rightarrow 23/2^-$
	4785	277	1162	$0.72 \pm 0.20$	$\sim -1.0$	–	$27/2^- \rightarrow 27/2^-$
	6052	886	999	$1.01 \pm 0.32$	$(E2)$	–	$(33/2^-) \rightarrow 29/2^-$

<sup>a</sup>DCO ratio for both  $\gamma$ -rays in the band with the same energy.

transitions in this band up to 932 keV are found to be  $M1 + E2$  in nature from the present PDCO measurements and the  $\delta$  values indicate significant  $E2$  admixtures (Table I). Hence, firm  $J^\pi$  values of  $23/2^-$ ,  $25/2^-$ ,  $27/2^-$ , and  $29/2^-$  are assigned for the 3553, 4167, 4785, and 5717 keV states, respectively. Interestingly, the  $\gamma$ -ray multipole mixing ratios

for the 379, 614, and 617 keV transitions are all found to be negative. Reliable DCO or PDCO measurements could not be performed for the 707, 834, and 1040 keV  $\gamma$ -rays at the top of the band owing to inadequate data statistics.

The 5166 keV level that feeds the 4167 keV state in Band 2 is assigned a spin of  $29/2^-$  on the basis of the

 TABLE II. Present experimental results on mean lifetime ( $\tau$ ),  $B(E2)$  rates, transition quadrupole moments ( $Q_t$ ), and quadrupole deformation ( $\beta_2$ ) for Band 3 in  $^{113}\text{Sb}$ .

$E_x$ (keV)	$E_\gamma$ (keV)	spin $J_i^\pi \rightarrow J_f^\pi$	$\tau$ (ps)	$B(E2)$ (W.u.)	$Q_t$ (eb)	$\beta_2$
3779	565	$23/2^- \rightarrow 19/2^-$	$1.34 \pm 0.18$	$330^{+52}_{-39}$	$5.58 \pm 0.53$	$0.37^{+0.03}_{-0.04}$
4461	682	$27/2^- \rightarrow 23/2^-$	$0.84 \pm 0.08$	$205^{+21}_{-18}$	$4.36 \pm 0.22$	$0.30^{+0.02}_{-0.03}$
5240	779	$31/2^- \rightarrow 27/2^-$	$0.38^{+0.07}_{-0.08}$	$232^{+62}_{-36}$	$4.61 \pm 0.50$	$0.31 \pm 0.03$
6095	855	$35/2^- \rightarrow 31/2^-$	$0.23 \pm 0.02$	$241^{+25}_{-19}$	$4.66 \pm 0.61$	$0.32 \pm 0.04$
7014	919	$39/2^- \rightarrow 35/2^-$	$0.18^{+0.04}_{-0.03}$	$215^{+43}_{-39}$	$4.40 \pm 0.50$	$0.30 \pm 0.03$
8000	986	$43/2^- \rightarrow 39/2^-$	$0.08 \pm 0.02$	$340^{+114}_{-68}$	$5.63 \pm 0.71$	$0.37^{+0.04}_{-0.05}$
9063	1063	$47/2^- \rightarrow 43/2^-$	$0.07^{+0.02}_{-0.01}$	$267^{+44}_{-60}$	$4.79 \pm 0.49$	$0.32^{+0.04}_{-0.03}$
10217	1154	$51/2^- \rightarrow 47/2^-$	$0.07^{+0.03}_{-0.02}$	$176^{+70}_{-53}$	$4.10 \pm 0.70$	$0.28 \pm 0.05$



adopted quadrupole multipolarity for the 999 keV  $\gamma$ -ray [12]. A tentative spin of  $(33/2^-)$  is proposed for the 6052 keV level from the present DCO ratio for the 886 keV  $\gamma$ -ray (Table I), considering the large error in the  $R_{\text{DCO}}$  value.

### C. Band 3

Band 3 is a  $\Delta J = 2$  intruder rotational sequence first reported by Janzen *et al.* [2] up to a spin of  $75/2^-$  (tentatively up to  $79/2^-$ ). Subsequently, the band was observed only up to  $59/2^-$  by Moon *et al.* [10]. The present group has also studied this band previously using the reaction  $^{100}\text{Mo}(^{20}\text{Ne}, p6n)$  at  $E = 136$  MeV [3] but states above  $J^\pi = 59/2^-$  could not be confirmed. The present work confirms all states up to  $67/2^-$  (Fig. 1). Figure 3(b) shows the sum of the  $90^\circ$  spectra gated by the lower-lying transitions in the band with energies up to 855 keV. In addition, two higher-energy states with excitation energies of 17369 and 19146 keV (Fig. 1) and decaying through the 1650 and 1777 keV transitions, respectively, are tentatively proposed to extend this band up to a spin of  $75/2^-$ . It may be noted here that the energies of the two highest transitions are significantly different compared to those reported by Janzen *et al.* [2].

Although the average transition quadrupole moment  $Q_t$  and deformation  $\beta_2$  of the states of Band 3 have been previously reported from a fitting of the fractional Doppler shifts [2], there is no report of the lifetimes of the individual states in the literature. Mean lifetimes of five states with energies 4461, 5240, 6095, 7014, and 8000 keV and a lower limit of mean life for the 9063 keV state have been previously reported by this group [3]. In the present work, lifetimes of all these states have been remeasured from the DSA data. In addition, new lifetime results of  $\tau = 1.34 \pm 0.18$ ,  $0.07^{+0.02}_{-0.01}$ , and  $0.07^{+0.03}_{-0.02}$  ps have been obtained for the 3779, 9063, and 10217 keV states, respectively, in the present work. Representative Doppler broadened line shapes for the 855, 986, and 1154 keV  $\gamma$ -rays depopulating the 6095, 8000, and 10217 keV states, respectively, are shown in Fig. 4 at  $90^\circ$

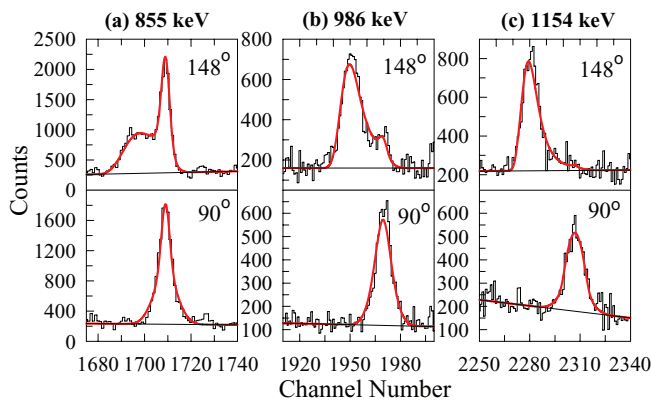


FIG. 4. (Color online) Gated DSA spectra for (a) 855 keV, (b) 986 keV, and (c) 1154 keV transitions belonging to Band 3. The top (bottom) panel shows spectra projected at  $148^\circ$  ( $90^\circ$ ) to the beam direction. Continuous lines are fits to the experimental data using the code LINESHAPE (see text).

and  $148^\circ$  to the beam direction. The present results for the transition quadrupole moments  $Q_t$ , summarized in Table II, are in general agreement with those reported earlier [3] within experimental errors. The average  $Q_t = 4.77 \pm 0.50$  obtained in this work for the eight states up to 10217 keV is consistent with our earlier result for five states [3] and also with that reported by Janzen *et al.* [2] within errors.

### D. Band 4

Excited negative parity  $\Delta J = 1$  bands have been observed in odd- $A$  Sb isotopes with  $A = 111$ –119. In  $^{113}\text{Sb}$ , the band was first reported by Moon *et al.* [10] up to a spin of  $(41/2^-)$ . The band has been extended in this work and its decay out to the states of Band 2 has been studied on the basis of the present coincidence data. It is observed that the 4347 keV bandhead decays into the  $21/2^-$ , 3174 keV state of Band 2 through the 3346 keV level somewhat differently compared to that reported in Ref. [10]. The 4347 keV state was shown to decay to the 3174 keV level through two branches, one of which consisted of the 1000.4 keV  $\gamma$ -ray followed by the 171.5 keV transition and the other composed of the 998.9 keV transition first and then the 173.0 keV  $\gamma$ -ray (energies as in Fig. 2 in Ref. [10]). In the present work, gates on the 129 and 419 keV  $\gamma$ -rays, belonging to Band 2 and lying immediately below the two decay branches (Ref. [10]), show a strong 172 keV transition but only a weak 298 keV  $\gamma$ -ray (belonging to Band 4). Indeed, all  $\gamma$ -rays belonging to Band 4 appear weak in these two gates. The latter  $\gamma$ -rays are nevertheless very strong in the spectrum gated by the combined 172 and 173 keV transitions that were placed immediately above the 419 and 129 keV  $\gamma$ -rays. These observations are clearly inconsistent with the decay scheme reported earlier [10]. The level scheme in the present work is revised as shown in Fig. 1 on the basis of the above observations where the 173 keV transition is placed immediately below the bandhead state. Also, the 419 keV transition is observed to be very strong in the combined 172 + 173 keV gate but rather weak in the spectrum gated by the 298 keV transition. This suggests that both 999 and 1001 keV  $\gamma$ -rays are weak while the 172 and 173 keV transitions are strong in nature.

Band 4 has been extended by the addition of the 515 and 996 keV transitions up to an excitation energy of 8544 keV and a tentative spin of  $(45/2^-)$ . A gate on the new 515 keV  $\gamma$ -ray [Fig. 3(c)] shows all the lower-lying transitions in the band. The 372, 391, and 469 keV  $\gamma$ -rays in this gated spectrum are stronger than the other  $\gamma$ -rays in the band as transitions with similar energies are also present in  $^{114}\text{Sb}$  along with a 516 keV  $\gamma$ -ray. The 996 keV crossover transition is weak and is observed only in the sum of the spectra gated by the lower-lying transitions. There is also a weak evidence for a 471 keV crossover transition (placed tentatively) connecting the  $27/2^-$  and  $23/2^-$  states. Confirmation of this  $\gamma$ -ray would suggest that the bandhead is probably at  $23/2^-$  and not  $25/2^-$  (Fig. 1).

The spin of the 3346 keV state, to which the 4347 keV bandhead state decays, is previously reported to be  $(21/2^-)$  [10]. The DCO ratio of  $0.73 \pm 0.10$  for the 172 keV  $\gamma$ -ray, determined from gating on the 419 keV  $E2$  transition, gives

$\delta = 0.17 \pm 0.10$ , suggesting that the transition is dipole in nature and that the possible spin values for the 3346 keV state are  $J^\pi = 23/2^-$  and  $19/2^-$ . However,  $19/2^-$  can be ruled out because the 1162 and 277 keV transitions (Fig. 1) are found to be quadrupole and dipole + quadrupole in nature, respectively (see Table I), suggesting that the 4508 keV state has a  $J^\pi = 27/2^-$  and the 277 keV  $\gamma$ -ray is a  $27/2^- \rightarrow 27/2^-$ ,  $M1 + E2$  mixed transition. A  $19/2^-$  assignment for the 3346 keV level requires that both 1162 and 277 keV  $\gamma$ -rays are quadrupole in nature as the  $J^\pi$  value for the 4785 keV level is confirmed to be  $27/2^-$ . A quadrupole assignment for the 277 keV transition would lead to an unrealistically large  $M3$  admixture for the  $\gamma$ -ray. The DCO ratio for the 1001 keV transition, feeding the 3346 keV state, indicates that the  $\gamma$ -ray is almost pure dipole in nature, as suggested in Ref. [10]. The 4347 keV state is therefore assigned a spin of  $25/2^-$ . A  $J^\pi$  of  $27/2^-$  is proposed for the 4645 keV level on the basis of the adopted dipole multipolarity for the 298 keV  $\gamma$ -ray [12]. The DCO ratios for the 372, 377, 391, and 414 keV transitions are all consistent with their dipole nature (Table I) leading to firm spin assignments for states up to 6199 keV. The  $J^\pi$  values for the higher-energy states in this band are shown as tentative in the absence of reliable DCO results.

#### IV. DISCUSSION

The low-energy states in  $^{113}\text{Sb}$  have been interpreted [10] as arising owing to the coupling of the odd proton in the  $d_{5/2}$ ,  $g_{7/2}$ , and  $h_{11/2}$  orbitals to  $0^+$  and  $2^+$  states of  $^{112}\text{Sn}$ .

Band 1 is the only known positive-parity band in  $^{113}\text{Sb}$ . This strongly coupled high- $K$  ( $K = 9/2$ ) band is built upon the  $9/2^+$  state that has the  $2p$ - $1h$  configuration  $\pi(g_{7/2})^2 \otimes \pi(g_{9/2})^{-1}$ . The excited states in the band decay through a cascade of strong  $\Delta J = 1$   $\gamma$ -rays with significant  $E2$  admixtures ( $\leq 15\%$ ) and weak crossover  $E2$  transitions. As expected for high- $K$  sequences, the band does not show appreciable signature splitting. An abrupt backbending occurs at a rotational frequency  $\hbar\omega \sim 0.4$  MeV, associated with an aligned spin of  $7\hbar$ – $8\hbar$ , owing to the alignment of a pair of  $\nu(h_{11/2})$  neutrons.

Potential energy surface calculations by Heyde *et al.* [13] for several odd- $A$  Sb isotopes predict a deformed minimum owing to a proton hole in the  $9/2^+[404]$  orbital. These calculations signify that the bands have a rotational character although the predicted deformations are small. The positive sign of the experimental mixing ratios for the  $\Delta J = 1$  transitions, obtained in the present work, suggest that the states belonging to Band 1 have a prolate deformation. The deformations could not be estimated experimentally as the Doppler shifts in the  $\gamma$ -rays deexciting the excited states are too small for a measurement of the level lifetimes. However, the experimental ratios of the reduced magnetic dipole and electric quadrupole transitions rates, given by

$$\begin{aligned}
 & \frac{B(M1; J \rightarrow J-1)}{B(E2; J \rightarrow J-2)} \\
 &= 0.697 \frac{E_\gamma^5(J \rightarrow J-2)}{E_\gamma^3(J \rightarrow J-1)(1+\delta^2)} \frac{I_\gamma(J \rightarrow J-1)}{I_\gamma(J \rightarrow J-2)} \frac{\mu_N^2}{e^2 b^2},
 \end{aligned}$$

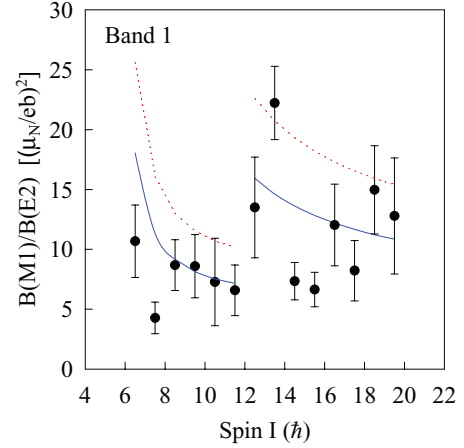


FIG. 5. (Color online) Experimental  $B(M1)/B(E2)$  ratios for states of Band 1 before and after the  $\nu(h_{11/2})$  alignment. Results of the Dönau-Frauendorf geometrical calculations are shown as continuous lines for  $\pi(g_{9/2})^{-1}$  and  $\pi(g_{9/2})^{-1} \otimes \nu(h_{11/2})^2$  configurations before and after the alignment corresponding to  $\beta_2 = 0.20$  and  $\gamma = 0^\circ$ . The broken lines show the geometrical model predictions for  $\beta_2 = 0.20$  and  $\gamma = 13^\circ$ . The inputs to the model calculations are given in the text.

where  $I$  and  $J$  refer to relative intensities and level spin, respectively, and  $E_\gamma$  is expressed in MeV, have been compared with the results of the Dönau-Frauendorf semiclassical calculations [14,15] and presented in Fig. 5. The  $g$  factors used in these calculations are  $g^{(1)}(\pi g_{9/2}) = 1.27$  and  $g^{(2)}(\nu h_{11/2}) = -0.21$  [16] where superscripts (1) and (2) refer to the configurations before and after alignment, respectively. The rotational  $g$  factor  $g_R = Z/A$  is 0.45. The alignments are taken to be  $i_x^{(1)} = 0$  and  $i_x^{(2)} = 7.5\hbar$  and  $K$ , the projection of the angular-momentum on the symmetry axis, is 4.5. Total Routhian surface (TRS) calculations, using a Woods-Saxon potential and monopole pairing [17], have been performed in this work. These calculations give a minimum in the energy at a quadrupole deformation  $\beta_2 = 0.20$  and  $\gamma = 13^\circ$ . The theoretical  $B(M1)/B(E2)$  ratios have been calculated for  $Q_o = 2.68$  eb (corresponding to  $\beta_2 = 0.20$  and  $\gamma = 0^\circ$ ) and  $Q_o = 2.25$  eb (for  $\beta_2 = 0.20$  and  $\gamma = 13^\circ$ ). Figure 5 shows that the experimental results are fairly well described by the model calculations for both  $\pi(g_{9/2})^{-1}$  and  $\pi(g_{9/2})^{-1} \otimes \nu(h_{11/2})^2$  configurations before and after the alignment, respectively, for  $\beta_2 = 0.20$  and  $\gamma = 0^\circ$  (continuous lines in Fig. 5). However, the calculated  $B(M1)/B(E2)$  ratios are consistently larger than the experimental ones by about 50% for  $\beta_2 = 0.20$  and  $\gamma = 13^\circ$  (shown by broken lines in Fig. 5) before alignment. Although there are relatively larger errors in the experimental ratios for states after the alignment, the calculated ratios corresponding to  $\beta_2 = 0.20$  and  $\gamma = 13^\circ$  are significantly large for most of the states. These results indicate that the states of Band 1 have a near axially symmetric, prolate deformed shape with a moderate quadrupole deformation of  $\beta_2 = 0.20$ .

The states of Band 2, built upon the  $19/2^-$  isomeric state, are connected by  $\Delta J = 1$  mixed  $M1 + E2$  transitions. Strongly coupled bands based on a single-quasiproton

configuration have a negative intrinsic quadrupole moment (corresponding to an oblate deformation) when the intraband transitions have a negative  $E2/M1$  mixing ratio, provided  $(g_K - g_R) > 0$ . The negative  $\delta_{E2/M1}$  values for the 379, 614, and 617 keV transitions appear to suggest an oblate deformation for the 3553, 4167, and 4785 keV states belonging to Band 2. It is plausible that the high- $\Omega$ , strongly downsloping in energy  $\pi h_{11/2}[505]11/2^-$  orbital comes near the proton Fermi surface for  $Z = 51$  and helps to stabilize the oblate shape and generate a sequence of  $\Delta J = 1$  transitions. The low-energy states of Band 2 do not show any signature splitting, as expected for bands built on a large- $\Omega$  orbital, while the energy staggering observed for states above  $J^\pi > 25/2^-$  possibly arise owing to the alignment of the  $h_{11/2}$  neutrons. However, such oblate bands have not been reported in any of the neighboring odd- $A$  Sb isotopes, although similar bands have been observed up to low spins in several iodine nuclei in the nearby mass region [18,19].

The negative parity Band 3 is identified with the intruder proton  $[550]1/2^-$  Nilsson orbital coupled to the deformed  $2p-2h$  state of  $^{112}\text{Sn}$ . Similar bands have been observed in all adjacent odd- $A$  Sb isotopes. In fact, three  $\Delta J = 2$  bands are reported in  $^{111}\text{Sb}$  although only one has a confirmed negative parity [20]. The parity of the other two bands is not known. In  $^{115}\text{Sb}$ , two negative-parity  $\Delta J = 2$  bands are reported, with the one built on the  $15/2^-$  state being identified to arise owing to the coupling of the odd proton in the  $h_{11/2}$  orbital to the known deformed  $2p-2h$  states of  $^{114}\text{Sn}$  [21]. However, none of these bands in  $^{111,115}\text{Sb}$  are as strongly deformed as the band (Band 3) in  $^{113}\text{Sb}$ . The large  $B(E2)$  values (see Table II) for the inband transitions in Band 3 correspond to an average transition quadrupole moment of  $Q_t = 4.77 \pm 0.50$  eb and quadrupole deformation  $\beta_2 = 0.32 \pm 0.03$ . The large deformation may be attributed to the occupation of the deformation driving  $h_{11/2}$  orbital by the odd proton, the deformation of the core states in  $^{112}\text{Sn}$ , and the strong proton-neutron interaction arising from the occupation of the same high- $j$   $h_{11/2}$  orbital by both the valence proton and the neutrons. Indeed, evidence of the strong  $pn$  interaction has been previously discussed by Janzen *et al.* [2].

Figure 6 shows a plot of the quadrupole moment  $Q_t$  as a function of level spin for Band 3. The plot provides an indication of the  $\nu h_{11/2}$  alignment that occurs at a rotational frequency of  $\hbar\omega = 0.46$  MeV. The dynamic moment of inertia  $\zeta^{(2)}$  for the band shows a second alignment at 0.69 MeV, associated with the rotational alignment of  $g_{7/2}$  protons. Following this alignment, the  $\zeta^{(2)}$  values decrease to about  $25\hbar^2 \text{ MeV}^{-1}$  for the highest observed state [2]. Furthermore, Fig. 6 shows that the  $Q_t$  values show a decreasing trend for the 9063 and 10217 keV states following the first alignment, suggesting a reduction in collectivity. This is manifested in the  $B(E2)$  values for the 1063 and 1154 keV transitions deexciting the  $47/2^-$  and  $51/2^-$  states, respectively (Table II). Indeed such a reduction of the  $B(E2)$  values signals a possible termination of the band at high spins in a noncollective oblate state. An extension of the lifetime studies to higher spins, not permitted owing to limitations of data statistics in the present work, might lead to a more conclusive understanding of this phenomenon.

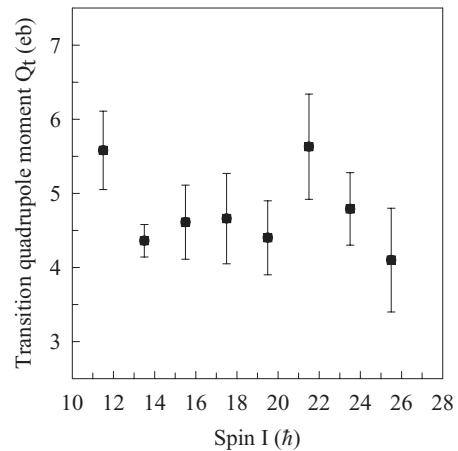


FIG. 6. Transition quadrupole moments plotted as a function of the level spin for Band 3.

Band 4 is a strongly coupled negative-parity sequence of prolate deformed states. The sign of the experimental  $\delta_{E2/M1}$  for the inband transitions (see Table I) supports a prolate deformation. Similar bands in  $^{115,117}\text{Sb}$  have been assigned the configuration  $\pi(g_{7/2})^2 \otimes \pi(g_{9/2})^{-1} \otimes \nu 7^-$ , where the  $\nu 7^-$  refers to the  $7^-$  state of the respective even-even Sn core. Moon *et al.* [10] have also proposed a similar configuration for this band. Lack of signature splitting and an absence of alignment is consistent with this configuration as it involves a proton hole in the high- $\Omega$   $g_{9/2}$  orbital and the  $7^-$  state of the core state involves a  $h_{11/2}$  neutron that blocks the  $\nu h_{11/2}$  alignment.

The short sequence of states (Band 5) built upon the 2308 keV level decays out strongly to Band 1 that has the dominant proton  $\pi(g_{7/2})^2 \otimes \pi(g_{9/2})^{-1}$  configuration. Besides, several transitions from Band 1 feed into the lower part of Band 5. These observations suggest that the two bands have a large overlap in their configurations. It is possible that the  $2p-1h$  weakly deformed low-energy states of Band 1 and those belonging to Band 5 allow for the coupling of vibration like levels with the rotational states. A similar admixing of vibrational levels with rotational states have been previously reported for  $^{111}\text{Sb}$  to explain the complicated decay of the  $2p-1h$  band into several low-energy states [20].

## V. CONCLUSION

Rotational bands in  $^{113}\text{Sb}$  have been studied using the reaction  $^{100}\text{Mo}(^{19}\text{F},6n)$  at a beam energy of 105 MeV. Two previously reported strongly coupled high- $K$  bands (Bands 1 and 4) involving the  $\pi g_{9/2}$  configuration have been extended. A new sequence of five states (Band 5), linked to Band 1 through interband transitions, is proposed. Spins and parities of several states have been inferred from DCO and  $\gamma$ -ray polarization studies. A comparison of the experimental  $B(M1)/B(E2)$  ratios with the Dönau-Frauentorf semiclassical calculations suggests that the states of Band 1 have a moderate quadrupole deformation of  $\beta_2 = 0.20$  with axial symmetry. Based on the negative  $E2/M1$  mixing ratios, low-energy states of Band 2 up



to 4785 keV are proposed to have an oblate deformation. The band has a negative parity and could arise from the occupation of the odd-proton in the high- $\Omega$   $h_{11/2}$  orbital. The intruder decoupled band (Band 3) has been studied up to a spin of  $67/2^-$  (tentatively up to  $75/2^-$ ). Mean lifetimes for eight states belonging to this band, involving a proton in the low- $\Omega$   $h_{11/2}$  orbital coupled to the deformed 2p-2h states of  $^{112}\text{Sn}$ , have been measured from the DSA data. These results suggest a large average quadrupole deformation of  $\beta_2 = 0.32 \pm 0.03$  for states up to an excitation energy of 10217 keV. The decrease in the reduced transition probabilities  $B(E2)$  for the  $47/2^-$  and  $51/2^-$  states is interpreted as owing to a possible termination of the band at high spin in a noncollective oblate state.

## ACKNOWLEDGMENTS

The authors thank the Indian National Gamma Array collaboration for setting up the array of clover detectors at the Inter University Accelerator Centre (IUAC), New Delhi. They also thank Dr. Amit Roy of the IUAC for providing the necessary facilities for the work. The assistance provided by the Pelletron operating staff is acknowledged. Thanks are due to Ajoy Mitra of the Saha Institute of Nuclear Physics, Kolkata, for help during the experiment and to Md. Eqbal of the Variable Energy Cyclotron Centre, Kolkata, for preparing the targets. One of the authors (S.G.) acknowledges with thanks the financial support provided by the UGC-DAE-CSR-KC vide Project No. UGC-DAE-CSR-KC/CRS/2009/NP05/1353.

- 
- [1] D. R. LaFosse, D. B. Fossan, J. R. Hughes, Y. Liang, P. Vaska, M. P. Waring, and J.-y. Zhang, *Phys. Rev. Lett.* **69**, 1332 (1992).
- [2] V. P. Janzen, H. R. Andrews, B. Haas, D. C. Radford, D. Ward, A. Omar, D. Prévost, M. Sawicki, P. Unrau, J. C. Waddington, T. E. Drake, A. Galindo-Uribarri, and R. Wyss, *Phys. Rev. Lett.* **70**, 1065 (1993).
- [3] S. Ganguly, P. Banerjee, A. Dey, and S. Bhattacharya, *Pramana* **77**, 277 (2011).
- [4] R. Wadsworth, R. M. Clark, J. A. Cameron, D. B. Fossan, I. M. Hibbert, V. P. Janzen, R. Krücken, G. J. Lane, I. Y. Lee, A. O. Macchiavelli, C. M. Parry, J. M. Sears, J. F. Smith, A. V. Afanasjev, and I. Ragnarsson, *Phys. Rev. Lett.* **80**, 1174 (1998).
- [5] P. Banerjee, S. Ganguly, M. K. Pradhan, H. P. Sharma, S. Muralithar, R. P. Singh, and R. K. Bhowmik, *Phys. Rev. C* **83**, 024316 (2011).
- [6] R. K. Bhowmik, INGASORT Manual (private communication).
- [7] D. C. Radford, *Nucl. Instrum. Methods Phys. Res., Sect. A* **361**, 297 (1995).
- [8] J. C. Wells and N. R. Johnson, *LINESHAPE: A Computer Program for Doppler-Broadened Lineshape Analysis*, ORNL Physics Division Progress Report for period ending September 30, 1991, No. ORNL-6689.
- [9] L. C. Northcliffe and R. F. Schilling, *Nucl. Data Tables* **7**, 233 (1970).
- [10] C.-B. Moon, C. S. Lee, J. C. Kim, J. H. Ha, T. Komatsubara, T. Shizuma, K. Uchiyama, K. Matsuura, M. Murasaki, Y. Sasaki, H. Takahashi, Y. Tokita, and K. Furuno, *Phys. Rev. C* **58**, 1833 (1998).
- [11] R. E. Shroy, A. K. Gaigalas, G. Schatz and D. B. Fossan, *Phys. Rev. C* **19**, 1324 (1979).
- [12] J. Blachot, *Nucl. Data Sheets* **100**, 179 (2003); **104**, 791 (2005); **111**, 1471 (2010).
- [13] K. Heyde, M. Waroquier, H. Vincx, and P. Van Isacker, *Phys. Lett. B* **64**, 135 (1976).
- [14] F. Dönau, *Nucl. Phys. A* **471**, 469 (1987).
- [15] P. H. Regan, A. E. Stuchbery, G. D. Dracoulis, A. P. Byrne, G. J. Lane, T. Kibédi, D. C. Radford, A. Galindo-Uribarri, V. P. Janzen, D. Ward, S. M. Mullins, G. Hackman, J. H. DeGraaf, M. Cromaz, and S. Pillote, *Nucl. Phys. A* **586**, 351 (1995).
- [16] T. Lönnroth, S. Vajda, O. C. Kistner, and M. H. Rafailovich, *Z. Phys. A* **317**, 215 (1984).
- [17] W. Nazarewicz, R. Wyss, and A. Johnson, *Nucl. Phys. A* **503**, 285 (1989).
- [18] Y. Liang, R. Ma, E. S. Paul, N. Xu, D. B. Fossan, J.-y. Zhang, and F. Dönau, *Phys. Rev. Lett.* **64**, 29 (1990).
- [19] Hariprakash Sharma, B. Sethi, P. Banerjee, Ranjana Goswami, R. K. Bhandari, and Jahan Singh, *Phys. Rev. C* **63**, 014313 (2000).
- [20] D. R. LaFosse, D. B. Fossan, J. R. Hughes, Y. Liang, H. Schnare, P. Vaska, M. P. Waring, J.-y. Zhang, R. M. Clark, R. Wadsworth, S. A. Forbes, E. S. Paul, V. P. Janzen, A. Galindo-Uribarri, D. C. Radford, D. Ward, S. M. Mullins, D. Prévost, and G. Zwartz, *Phys. Rev. C* **50**, 1819 (1994).
- [21] R. S. Chakravarthy and R. G. Pillay, *Phys. Rev. C* **54**, 2319 (1996).